Consistent boundary conditions for integrated LES/RANS simulations: LES outflow conditions

By J. U. Schlüter and H. Pitsch

1. Motivation

Numerical simulations of complex large-scale flow systems must capture a variety of physical phenomena in order to predict the flow accurately. Currently, many flow solvers are specialized to simulate one part of a flow system effectively, but are either inadequate or too expensive to be applied to a generic problem.

As an example, the flow through a gas turbine can be considered. In the compressor and the turbine section, the flow solver has to be able to handle the moving blades, model the wall turbulence, and predict the pressure and density distribution properly. This can be done by a flow solver based on the Reynolds-Averaged Navier-Stokes (RANS) approach. On the other hand, the flow in the combustion chamber is governed by large scale turbulence, chemical reactions, and the presence of fuel spray. Experience shows that these phenomena require an unsteady approach (Veynante & Poinsot, 1996). Hence, the use of a Large-Eddy Simulation (LES) flow solver is desirable.

While many design problems of a single flow passage can be addressed by separate computations, only the simultaneous computation of all parts can guarantee the proper prediction of multi-component phenomena, such as compressor/combustor instability and combustor/turbine hot-streak migration. Therefore, a promising strategy to perform full aero-thermal simulations of gas-turbine engines is the use of a RANS flow solver for the compressor sections, an LES flow solver for the combustor, and again a RANS flow solver for the turbine section (Fig. 1).

2. Interface Treatment

The simultaneous computation of the flow in all parts of a gas turbine with different flow solvers requires an exchange of information at the interfaces of the computational domains of each part. The necessity for information exchange in the flow direction from the upstream to the downstream flow solver is self-explanatory: the flow in a passage is strongly dependent on mass flux, velocity vectors, and temperature at the inlet of the domain. However, since the Navier-Stokes equations are elliptic in subsonic flow, the downstream flow conditions can have a substantial influence on the upstream flow development. This can easily be imagined by considering that, for instance, a flow blockage in the turbine section of the gas turbine can affect and even stop the flow through the entire engine. This means that the information exchange at each interface has to go in both, downstream *and* upstream, directions.

Considering an LES flow solver computing the flow in the combustor, information on the flow field has to be provided to the RANS flow solver computing the turbine as well as to the RANS flow solver computing the compressor, while at the same time, the LES solver has to obtain flow information from both RANS flow solvers (Fig. 2). The coupling can be done using overlapping computational domains for the LES and RANS

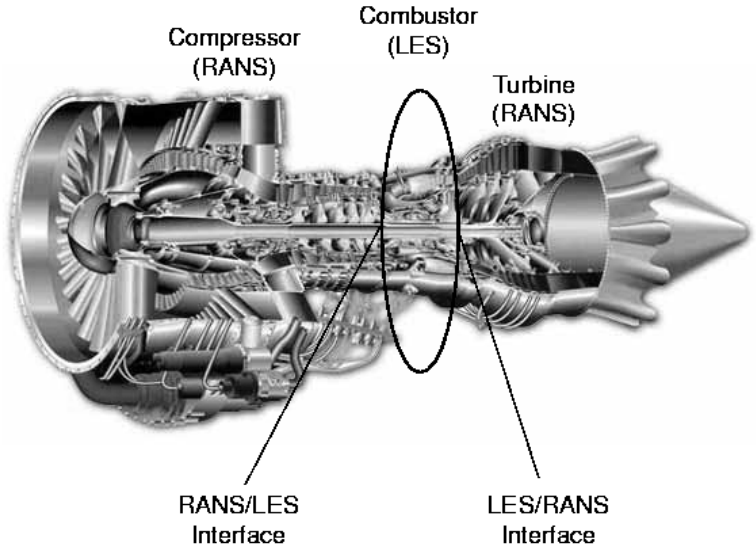

FIGURE 1. Gas turbine engine

simulations. For the example of the combustor/turbine interface this would imply that inflow conditions for RANS will be determined from the LES solution at the beginning of the overlap region, and correspondingly the outflow conditions for LES are determined from the RANS solution inside the overlap region.

However, the different mathematical approaches of the different flow solvers make the coupling of the flow solvers challenging. Since LES resolves large-scale turbulence in space and time, the time step between two iterations is relatively small. RANS flow solvers average all turbulent motions over time and predict ensemble averages of the flow. Even when a so-called unsteady RANS approach is used, the time step used by the RANS flow solver is still much larger than that for an LES flow solver.

The specification of boundary conditions for RANS from LES data is relatively straightforward. The LES data can be averaged over time and used as boundary condition for the RANS solver. The problem of specifying inflow conditions for LES from upstream RANS data is similar to specifying LES inflow conditions from experimental data, which is usually given in time averaged form, and has therefore been investigated in some detail. A method that has been successfully applied in the past, is, for instance, to generate a time-dependent database for inflow velocity profiles by performing a separate LES simulation, in which virtual body forces are applied to achieve the required time-averaged solution (Pierce & Moin, 1998b).

In the present study the remaining flux of information from a downstream RANS computation to an upstream LES computation is investigated. LES computations have already shown that the flow can be sensitive to the outflow conditions (Moin, 1997, Pierce & Moin, 1998a). The outflow conditions for LES have to be specified such that the time-averaged mean values of all computed quantities match the RANS solution at a given plane, but the instantaneous solution at the outflow still preserves the turbulent fluctuations.

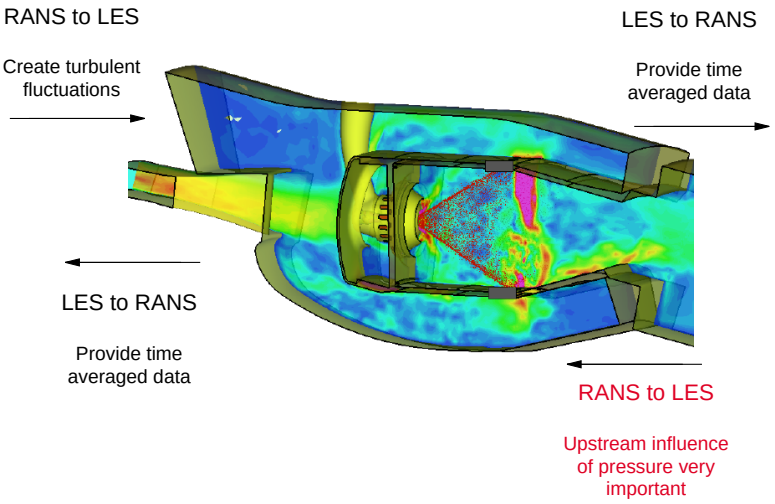

FIGURE 2. Gas turbine combustor with interfaces

3. Formulation of the outflow boundary treatment

Modern LES flow solvers are often based on a low-Mach-number formulation. With this approximation, acoustic pressure fluctuations are neglected and the hydrodynamic pressure variations are determined by a Poisson equation. This formulation makes it impossible to prescribe the pressure at the outlet of the LES domain directly. Instead, only the velocities or their derivatives can be specified as boundary conditions in the LES flow solver, and the pressure adjusts accordingly. The mean velocity profiles are enforced by adding a virtual body force to the right-hand side of the momentum equations inside the overlap region of the computational domains of the LES and the RANS flow solver. For a constant-density flow which is stationary in the mean, the body force is given by

$$F_i(\boldsymbol{x}) = \frac{1}{\tau_{\mathrm{F}}}(\bar{u}_{i,\mathrm{RANS}}(\boldsymbol{x}) - \bar{u}_{i,\mathrm{LES}}(\boldsymbol{x}))\,, \tag{3.1}$$

where $\bar{u}_{i,\mathrm{RANS}}$ is the vector of target velocities obtained from the RANS computation and $\bar{u}_{i,\mathrm{LES}}$ is the vector of time-averaged velocities from the LES computation. The forcing time scale τ_{F} can, to first order, be determined from the bulk velocity u_{B} and the length of the forcing region l_{F} as $\tau_{\mathrm{F}} = l_{\mathrm{F}}/u_{\mathrm{B}}$. Experience shows that the forcing time is usually much lower than this estimate, so that this can serve as an upper limit. For numerical purposes a convective boundary condition is applied at the outlet plane of the LES domain.

The forcing term in Eq. (3.1) involves only mean velocities, while the corresponding momentum equation is solved for the instantaneous velocities. Thus the mean velocities from the LES simulation are corrected without attenuating the resolved turbulent fluctuations. It will be shown later that, to achieve this goal, the averaging time for $\bar{u}_{i,\mathrm{LES}}$ needs to be longer than the characteristic times of the turbulence. Equation (3.1) also shows that the forcing term tends to zero if the actual mean velocity from the LES approaches the target velocity, which is a consistency requirement. Note also that the RANS velocities are prescribed not only in one plane, but in the entire overlap region.

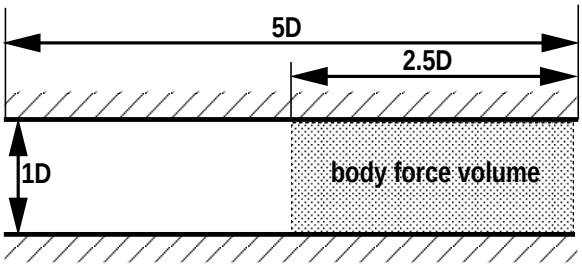

FIGURE 3. Geometry of the pipe geometry

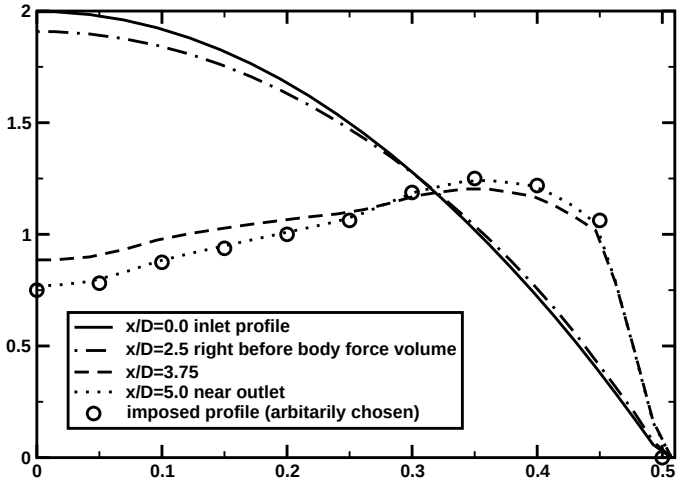

FIGURE 4. Laminar pipe flow: radial profiles of axial velocity component $\bar{u}_x$

4. LES Flow Solver

For the current investigation, the LES flow solver developed at the Center for Turbulence Research (Pierce & Moin, 1998a) has been used. The flow solver solves the filtered momentum equations with a low-Mach-number assumption on an axisymmetric structured mesh. A second-order finite-volume scheme on a staggered grid is used (Akselvoll & Moin, 1996).

The subgrid stresses are approximated with an eddy-viscosity approach. The eddy viscosity is determined by a dynamic procedure (Germano *et al*, 1991; Moin *et al*, 1991).

5. Numerical experiment: pipe-flow geometry

In order to prove the feasibility and the well-posedness of this approach a pipe flow has been computed (Fig. 3). The pipe has a length of five times the diameter D and the virtual body force is applied in a volume of length $2.5\,D$ at the end of the pipe flow. The mesh consists of $128\times32\times64$ cells.

As a first step, a laminar pipe flow at a Reynolds number Re=1000 is considered. Fig. 4 shows the resulting velocity profiles. The solid line shows the parabolic inlet profile corresponding to the solution of a fully-developed pipe flow. Without forcing, this would be the solution at any downstream location in the pipe. The circles denote an arbitrarily-chosen velocity profile, with the same mass flow rate as the inlet profile, which is to be

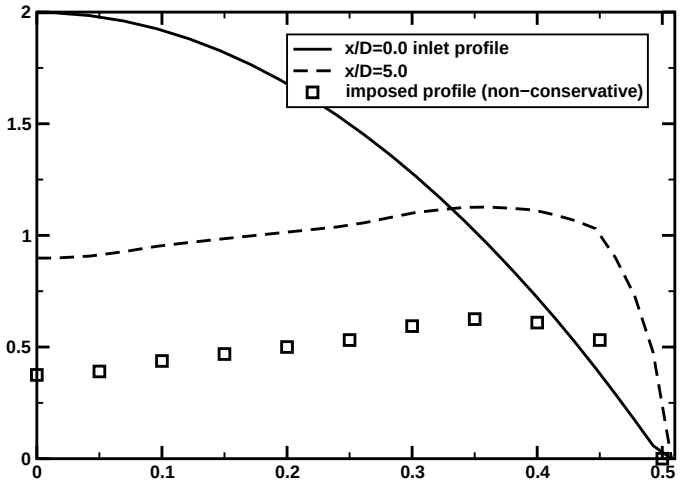

FIGURE 5. Laminar pipe flow with non-conservative velocity profile imposed

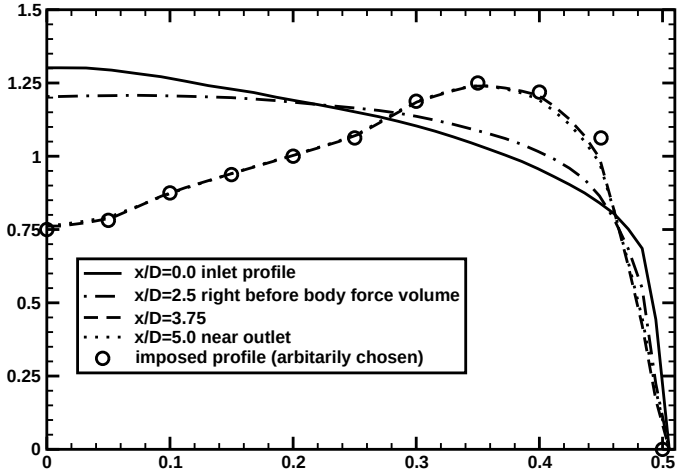

FIGURE 6. Turbulent pipe flow, radial profiles of axial velocity component $\bar{u}_x$

matched at the outlet. The dash-dotted line is a profile just upstream of the forcing region. The profile is different from the inflow solution, indicating that forcing influences the flow field even upstream of the forcing region. After applying the virtual body force, the computed velocity profile quickly converges towards the imposed velocity profile.

An important test for consistency and well-posedness is the enforcement of a velocity profile which does not conserve mass. The exchange of the velocity profiles between RANS and LES flow solver may introduce numerical errors, especially due to the interpolation between two different meshes, which could accumulate over time. In order to investigate the behavior of the proposed LES outflow conditions when encountering this problem, an additional computation was made, where a "non-conservative" velocity profile, with a different mass flow rate, was enforced. Fig. 5 shows the resulting velocity profiles. The squares denote the imposed velocity profile, which clearly underestimates the mass flux. However, the computed velocity profile at the end of the forcing region has the same

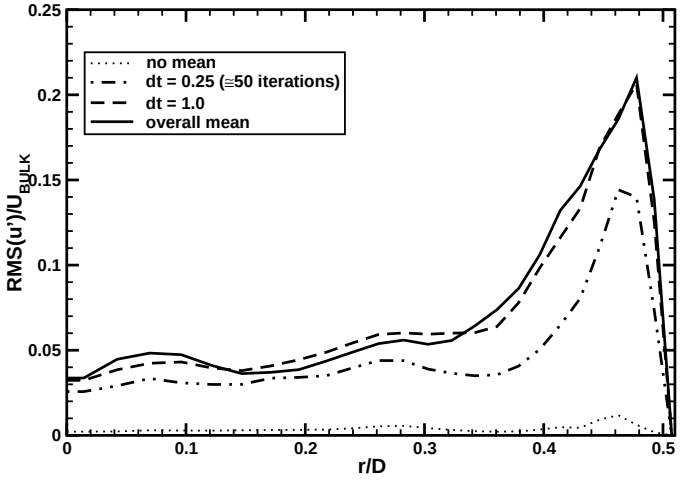

FIGURE 7. Turbulent pipe flow: radial profiles of axial velocity fluctuations $\sqrt{\overline{u'^2}}$ for different averaging time-span

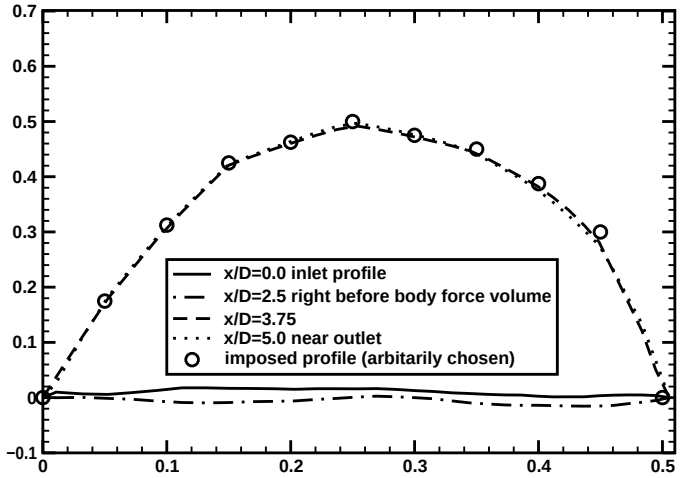

FIGURE 8. Turbulent pipe flow, radial profiles of azimuthal velocity component $\bar{u}_\phi$

mass flux as the inlet profile. This shows that the method is robust against inaccuracies resulting from the exchange of velocity profiles.

The next test case considered here is a turbulent pipe flow at a Reynolds number Re = 15000. Applying the proposed correction of the LES outflow by virtual body forces to this problem leads to the question of how to define the mean value $\bar{u}_{\mathrm{LES}}$ of the LES computation. Several approaches have been tested:

(a) Using the actual velocity $\bar{u}_{\mathrm{LES}} = u(t)$. This results in a strong damping of turbulent fluctuations, since fluctuations of the velocity obviously lead to a counteracting virtual body force.

(b) Using the overall mean value $\bar{u}_{\mathrm{LES}} = \frac{1}{t-t_0} \int_{t_0}^{t} \bar{u}\, dt$. This ensures the least interference with turbulent fluctuations, but does not allow for unsteadiness in the mean profiles.

(c) Averaging over a trailing time window $\bar{u}_{\mathrm{LES}} = \frac{1}{\Delta t} \int_{t-\Delta t}^{t} \bar{u}\, dt$. Here it has to be ensured that Δt is long enough to average the turbulent fluctuations, but short enough to allow for unsteadiness of the mean profiles.

All approaches result in the same mean velocity field (Fig. 6). Since the turbulent velocity profile is already closer to the imposed profile than in the laminar case, the flow field converges faster towards the imposed profile. However, there are some remarkable differences in the turbulent fluctuations.

Fig. 7 shows the profiles of the axial velocity fluctuations for different averaging time-spans. Using approach (a) results in complete attenuation of the turbulence. Assuming that an overall mean value (approach (b)) preserves the turbulence, it can be seen that the averaging time has to be sufficiently long to prevent attenuation of the turbulence. Here, averaging over one non-dimensional time unit, given by the ratio of pipe diameter to bulk velocity, was found to be sufficient. This seems reasonable, since the abovementioned criteria require the averaging time to be of the order of the Eulerian integral time scale of the turbulence, which for a turbulent pipe flow is proportional to the ratio of pipe diameter to bulk velocity.

For a swirling flow the same procedure can also applied to the azimuthal velocity component. Fig. 8 shows the profiles of the azimuthal velocity component. Again, the inflow conditions correspond to a fully-developed turbulent pipe without swirl and the virtual body force is applied as shown in Fig. 3. At the end of the forcing region the target profile is matched perfectly.

The results of the pipe-flow investigation demonstrate that the proposed treatment of the LES outflow conditions with virtual body forces can be used to enforce a mean flow solution at the LES outflow, and that the enforced outflow conditions can indeed alter the upstream flow field.

6. Validation: swirl combustor geometry

In order to validate the proposed method for treating LES outflow conditions for an LES/RANS interface, the method will be applied to a more complex configuration. The test case chosen is that of a swirling flow inside a combustor geometry with a swirl number, $S = 0.38$, with S defined as:

$$S = \frac{1}{R} \frac{\int_0^R r^2 \bar{u}_x \bar{u}_\phi \, dr}{\int_0^R r \bar{u}_x^2 \, dr}\,, \tag{6.1}$$

where u_x is the axial velocity component, u_ϕ the azimuthal velocity component, and R the radius of the nozzle. This swirl number has been chosen because it is slightly above the critical limit at which a central recirculation zone develops, where the flow is believed to be most sensitive to outer influences such as the outflow boundary conditions (Gupta *et al*, 1984; Dellenback *et al*, 1988). Swirl flows are dominated by large-scale turbulence making these flows a field of application of LES *par excellence*. LES usually achieves high levels of accuracy in predicting swirl flows (Pierce & Moin, 1998a; Schlüter *et al.*, 2001).

In order to demonstrate the importance of LES outflow conditions and to prove the ability of the proposed LES outflow treatment with virtual body forces to prescribe outflow conditions correctly, three different outflow geometries have been considered:

(a) a swirl flow with a contraction near the outlet at $x/D = 3.0$ (Fig. 9);

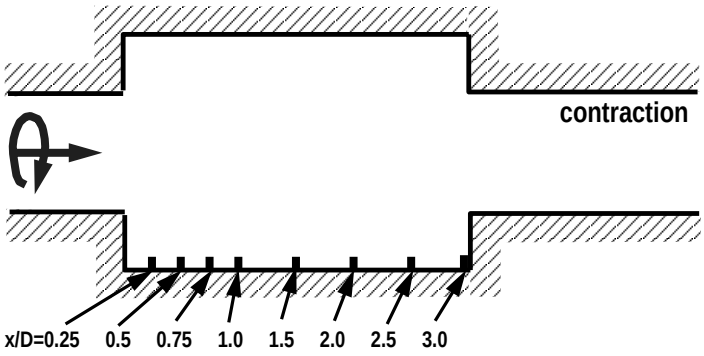

FIGURE 9. Swirl flow geometry with contraction

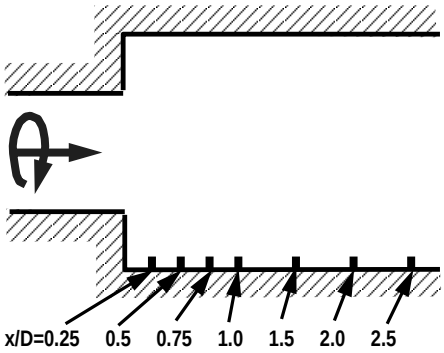

FIGURE 10. Reduced swirl flow geometry without virtual body force

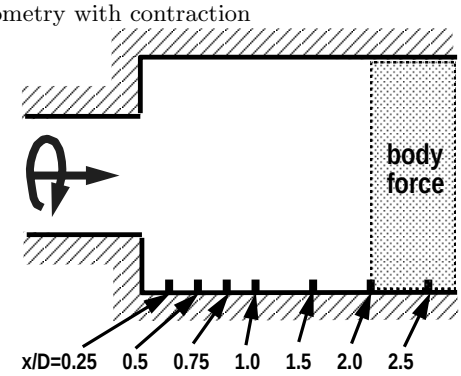

FIGURE 11. Reduced swirl flow geometry with virtual body force

(b) a swirl flow where the computational domain is cut off just upstream of the contraction of case (a) at $x/D = 2.75$ (Fig. 10);

(c) the same geometry as in case (b), but with the proposed boundary condition applied in order to simulate the effect of the contraction (Fig. 11).

The mesh size of geometry (a) consists of $384\times64\times64$ cells while the mesh of cases (b) and c) consists of $256\times64\times64$ cells. The point distribution of both meshes is the same, except for the contraction itself.

Case (a) will be considered as the reference case. Since the computational domain includes the contraction, its influence on the upstream flow will be correctly reflected in the LES solution. Assuming that the contraction is to be computed with a RANS code, in case (b) the computational domain has been reduced and the contraction is outside of the LES domain. Hence, its influence on the LES flow field is neglected in case (b).

Fig. 12 shows the mean velocity profiles in cases (a) and (b). It can be seen, that the velocity profiles of the computation with the reduced geometry (b) (dashed line) differ from the profiles of the computation of the full geometry (a) (solid line). Hence, it is apparent that the downstream geometry variation has a substantial influence on the entire domain, and that geometry (b) cannot be used to approximate the flow in geometry (a) without special boundary treatment.

In order to take the contraction outside of the computational domain into account, the proposed outflow boundary treatment is employed. The Reynolds-averaged velocity profiles from $x/D = 2.0 - 2.5$ from the LES computation of case (a) are imposed, with virtual body forces, on the reduced geometry. Fig. 12 shows the mean velocity profiles

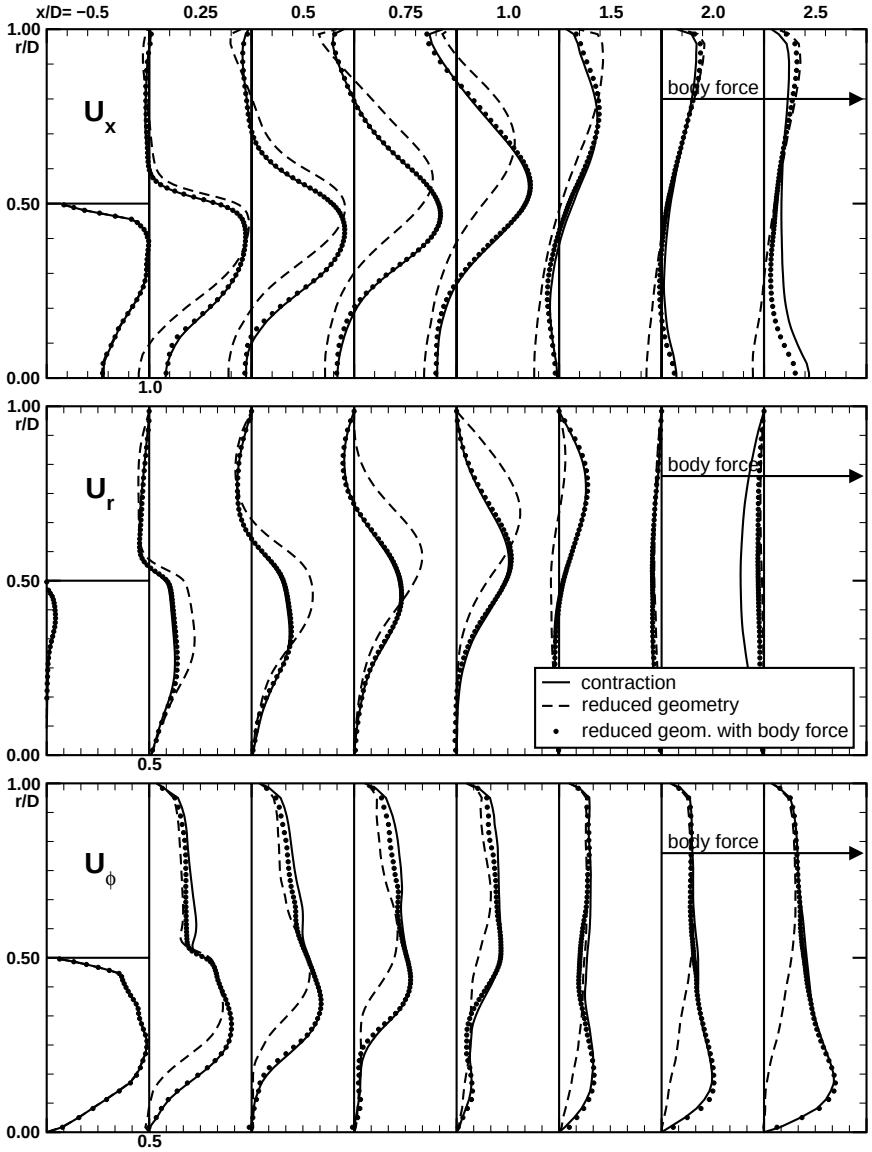

FIGURE 12. Velocity profiles for different axial locations; solid lines: contraction (case (*a*)); dashed lines: reduced geometry without virtual body force(case (*b*)); symbols: reduced geometry with virtual body force (case (*c*))

of case (*c*) (black dots). It can be seen that not only do the velocity profiles inside the virtual-body-force volume adjust, but so also do the velocity profiles upstream. The LES computation of the reduced geometry with the virtual body force delivers essentially the same prediction as the computation of the entire geometry.

The influence of the LES outflow condition on the velocity fluctuations is shown in Fig. 13. The different mean-velocity distribution due to the presence of a contraction results in a different turbulence distribution (compare solid line and dashed line in Fig. 13). The employment of the virtual body forces corrects not only the mean velocity field, but

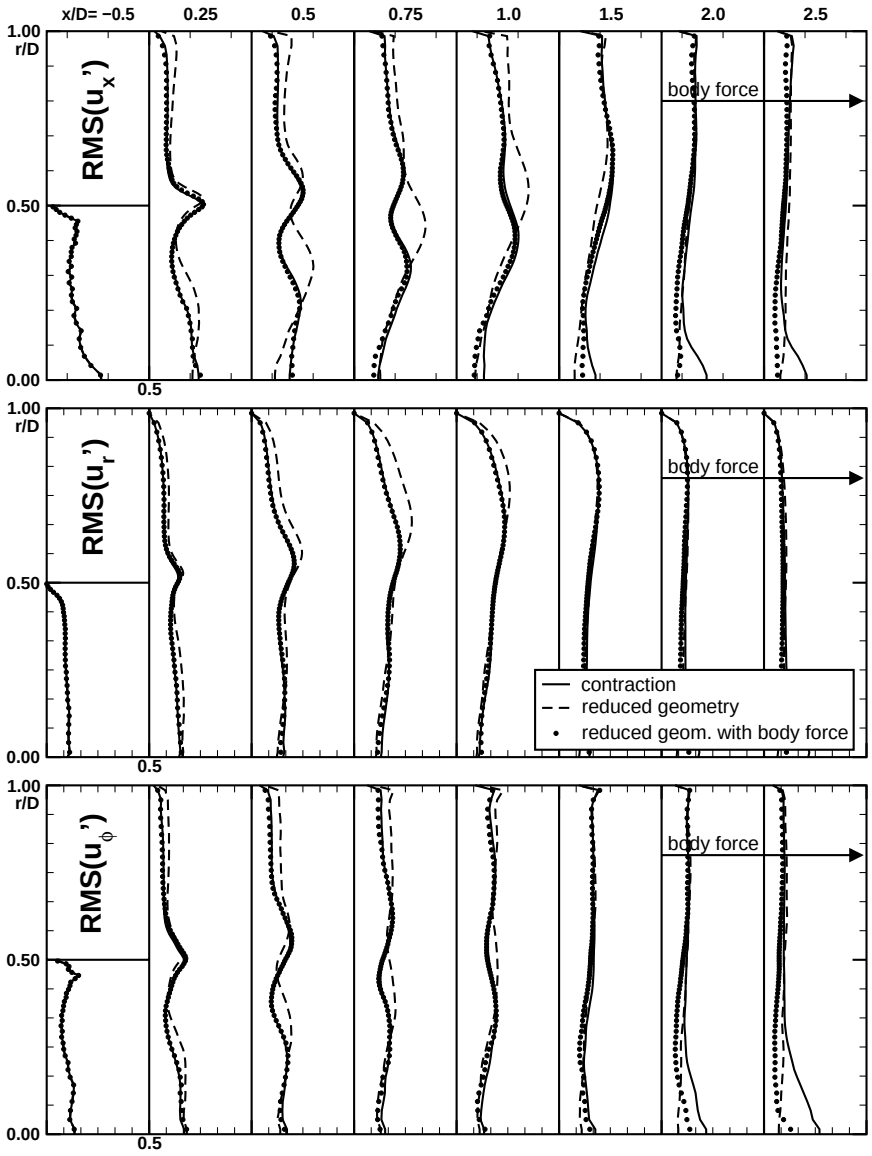

FIGURE 13. Profiles of velocity fluctuations for different axial locations; solid lines: contraction (case *(a)*); dashed lines: reduced geometry without virtual body force (case *(b)*); symbols: reduced geometry with virtual body force (case *(c)*)

also the turbulent quantities (compare solid line and filled circles in Fig. 13). The virtual body force results in an adjustment of the turbulent quantities so that the flow upstream of the body force volume is nearly indistinguishable from the complete computation with the contraction.

In Fig. 14, the axial pressure distribution on the axis is shown. Due to the variances in the flow fields of the cases *(a)* and *(b)*, especially in the extend and strength of the recirculation zone, the pressure distributions differ. Although the proposed outflow boundary adjustment by virtual body forces acts only on the velocity components and not

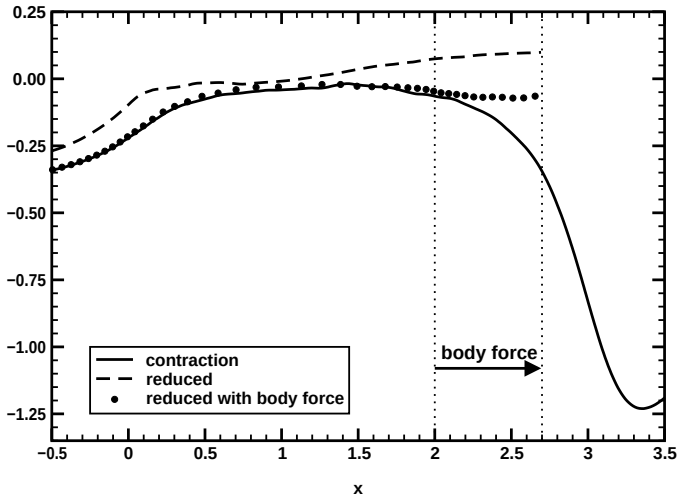

FIGURE 14. Axial pressure distribution on the axis; solid lines: contraction (case (*a*)); dashed lines: reduced geometry without virtual body force (case (*b*)); symbols: reduced geometry with virtual body force (case (*c*))

on the pressure itself, the pressure distribution adjusts to the modified outflow conditions. The pressure distributions in cases *(a)* and *(c)* are in agreement upstream of the body-force volume.

7. Conclusions

The results of this study show that the outflow conditions may have a major impact on the accuracy of LES computations. Hence, a proper description of the outflow conditions is mandatory.

To avoid the computation of the downstream geometry with LES a method has been proposed to correct the outflow conditions. This method ensures the adjustment of the LES flow field to the statistical data computed by a downstream RANS flow solver.

The adjustment of the LES outflow has an effect throughout the entire flow-field. The resulting prediction of the flow-field is nearly indistinguishable from an LES computation of the entire domain. This allows a drastic decrease in computational costs.

Future efforts will combine the LES flow solver with an actual RANS flow solver in a two-way-coupled LES/RANS simulations.

REFERENCES

AKSELVOLL, K., & MOIN, P. 1996 Large-eddy simulation of turbulent confined coannular jets. *J. Fluid Mech.* **315**, 387–411.

DELLENBACK, P. A., METZGER, D. E. & NEITZEL, G. P 1988 Measurements in turbulent swirling flow through an abrupt axisymmetric expansion. *AIAA J.* **26**, 669-681.

GERMANO, M., PIOMELLI, U., MOIN, P. & CABOT, W., 1991 A dynamic subgrid-scale eddy viscosity model. *Phys. Fluids A* **3**, 1760-1765.

GUPTA, A. K., LILLEY, D. G. & SYRED, N. 1984 *Swirl Flows.* Abacus Press.

Moin, P., Squires, K., Cabot, W. & Lee, S. 1991 A dynamic subgrid-scale model for compressible turbulence and scalar transport. *Phys. Fluids A* **3**, 2746-2757.

Moin, P. 1997 Progress in large eddy simulation of turbulent flows. *AIAA* Paper 97-0749.

Pierce, C. D. & Moin, P. 1998a Large eddy simulation of a confined coaxial jet with swirl and heat release. *AIAA* Paper 98-2892.

Pierce, C. D. & Moin, P. 1998b Method for generating equilibrium swirling inflow conditions. *AIAA J.* **36**, 1325-1327.

Schlüter, J., Schönfeld, T., Poinsot, T., Krebs, W. & Hoffmann, S. 2001 Characterization of confined swirl flows using large eddy simulations. *ASME* 2001-GT-0060

Veynante, D. & Poinsot, T. 1996 Reynolds averaged and large eddy simulation modeling for turbulent combustion. In *New Tools in Turbulence Modeling*, Springer, 105–140.